ELSEVIER

Journal of Physics and Chemistry of Solids 60 (1999) 407–414

JOURNAL OF PHYSICS AND CHEMISTRY OF SOLIDS

Thermal depolarization studies in leukolite (polycrystalline magnesite, $MgCO_3$)[1]

A.N. Papathanassiou

Department of Physics, Section of Solid State Physics, University of Athens, Panepistimiopolis, GR 157 84 Zografos, Athens, Greece

Received 29 October 1997; accepted 8 July 1998

Abstract

We performed thermally stimulated depolarization current experiments on leukolite (polycrystalline magnesite). Two bands appear in the thermograms: one is located at 140 K (LT1 band) and another one (HT band) that reaches a maximum around 305 K. In the present work, we perform the characterization of the HT band by carrying out successive TSDC scans with electrodes of different blocking degree by changing the polarization conditions and by varying the thickness of the specimen. The results indicate that the HT band is characterized by the distribution in the relaxation time and is related probably to the homogeneous polarization of the sample. The features can be interpreted through an interfacial polarization mechanism like the trapping of free charges at the grain boundaries. We performed the thermal sampling scheme and obtained a set of the constituents that build up the HT band. The fitting of a theoretical curve with normal distribution in the activation energy to the experimental data yielded the relaxation parameters. © 1999 Elsevier Science Ltd. All rights reserved.

Keywords: Ionic thermocurrent; D. Dielectric properties; D. Electrical properties; D. Transport properties

1. Introduction

Magnesite ($MgCO_3$), calcite ($CaCO_3$) and the mixed crystal dolomite ($CaMg(CO_3)_2$) constitute the calcite family [1]. They all share the rhombohedral crystal structure. To a very crude approximation, they are regarded as being typical ionic systems with the common sodium chloride structure; in the simplified NaCl picture, the divalent cation takes the place of the sodium anion and the carbonate group replaces the chlorine ion. However, the carbonate structure actually departs from the oversimplified situation mentioned above. The carbonate group is not a center of symmetry; in magnesite and calcite, the three oxygens are located at the corners of an equilateral triangle, and the carbon settles at its corner [2]. The stability of the mixed crystal dolomite requires slight distortions and deviations from this visualization. Another interesting point is that the ionic lattice accommodates carbonate groups with inherent covalent bonding. Recent calculations performed for magnesite showed that the bonding between the magnesium cation and the carbonate root has a small but considerable covalent constituent [3]. Thus, the carbonate salts exhibit structural characteristics which are more complicated than those of the most common ionic crystals.

Recently, we have presented a series of papers on the dielectric relaxation [4–7] and the transport properties [8,6] of the alkaline earth carbonate salts. Regarding the calcite family, we investigated the effect of the specific lattice type on the formation of certain polarizable defect centers (the defect structure establishment) [4,5,7]. The mixing of two ionic systems to a mixed crystal induces long- and short-range effects which affect the dynamics of the defect dipoles [9]. The long-range effect is related to the modification of the lattice spacing, which is caused by the mixing. The short-range effect represents the modification of the immediate environment of the rotating dipole [9]. By using the thermally stimulated depolarization current (TSDC) spectroscopy [10], we studied the aforementioned phenomena in calcite, dolomite and magnesite [4,7,6,5]. Finally, we studied the transport mechanisms, which operate in calcite [6] and dolomite [8]. For dolomite [11] and magnesite [12] we also performed conductivity experiments as a function of pressure, so as to identify the nature of the conduction mechanism and to understand the transport

[1] To the memory of Ioannis Koutsidis, who left so early.

0022-3697/99/$ - see front matter © 1999 Elsevier Science Ltd. All rights reserved.
PII: S0022-3697(98)00270-4

phenomena. The present work is part of our research program on carbonates and the objective is to conclude on the origin and the identity of the broad relaxation that activates at the room temperature region, by applying the TSDC technique [10], which operates at relatively low temperatures.

The results for the alkaline earth carbonates do not only aim to the development of pure research, as mentioned in the preceding paragraphs, but are highly desirable in the field of technological and industrial applications. Leukolite is a high-purity polycrystalline magnesium carbonate mineral, which is of considerable importance in the industry, for preparing refractory materials, cements, paper, rubber and pharmaceutical products. On the other hand, the carbonates are substantial participants of the earth's crust. Dielectric and electrical laboratory experiments are potentially significant for understanding and modelling the large scale geophysical electrical phenomena [13]. Additionally, our results are related to determine the mechanisms of charge flow and induced polarization resulting from natural or artificial sources in the earth's solid crust. The detection of dipole or extended dipole relaxation (i.e., interfacial polarization) is critical for the applicability of theoretical models which predict a polarization or depolarization dipole relaxation that accompany the pressurization of geomaterials and are actually precursors of seismic activity [13,14].

2. Theory

The polarization of an ionic dielectric under the action of an external electric field, consists of three main heterocharge components [15]: (i) the atomic and ionic polarization; (ii) the polarization of ionic dipoles existing in the matrix (like dipole defect); and (iii) the free charge transport polarization. The latter involves two phenomena: (a) the space charge polarization, when the moving charges are immobilized at the sample electrode interface; (b) the interfacial polarization, provided that the carriers are trapped in internal obstacles, like the interfaces separating the conductive inclusions and the non-conductive matrix, or the dislocations.

The dielectric relaxation is characterized by the relaxation time τ. A common assumption made is that the temperature dependence of the relaxation time obeys the following Arrhenius equation:

$$\tau(T) = \tau_0 \exp\left(\frac{E}{kT}\right) \tag{1}$$

where k is Boltzmann's constant, E denotes the activation energy and τ_0 is the pre-exponential factor.

The TSDC technique [10] is capable of detecting the dipole orientation and free charge transport polarization (cases (ii) and (iii)). We present the basic steps of the TSDC method in brief, focusing on the space charge polarization [15]: at the temperature T_p (usually room temperature, RT) we apply an electric field to the dielectric for the time interval t_p, which is usually much longer than the relaxation time $\tau(T_p)$ of the relaxation mechanism. The motion of free charges toward the sample's surfaces and their subsequent accumulation to the (non-ohmic) sample electrode interface, result in the polarization of the material. By keeping the electric field on, the sample is cooled to liquid nitrogen temperature (LNT). The relaxation time τ(LNT) at the LNT is practically infinite. Therefore, the polarization state attained during the polarizing stage, remains frozen, even when switching off the field. Subsequently, by heating the sample in the absence of the external field, the space charge polarization is annihilated at relatively high temperatures (usually around the RT) where the thermal energy is high enough to assist the spatial redistribution of the space charge. The time (equivalently, temperature) variation of the polarization is responsible for the depolarization current emitted. A sensitive electrometer connected to the sample surfaces during the heating procedure, records a transient thermal depolarization current $I(T)$, originating from the time variation of the space charge polarization.

For the simple case of rotating non-interacting dipoles, the signal $I_{dip}(T)$ is a glow curve like:

$$I_{dip}(T) = \frac{S\Pi_0}{\tau_0} \exp\left[-\frac{E}{kT} - \frac{1}{b\tau_0}\int_{T_0}^{T} \exp\left(-\frac{E}{kT}\right) dT\right] \tag{2}$$

where Π_0 is the initial polarization of the dielectric, S is the surface sample area which is in contact with each one of the electrodes, E is the activation energy of the rotating dipoles, b is the constant heating rate, and T_0 coincides to the LNT.

If the activation energy is not single valued, but has a normal distribution around E_0, with distribution function [16,17]

$$f(E) = \frac{1}{\sqrt{2\pi - \sigma}} \exp\left[-\frac{(E - E_0)^2}{2\sigma^2}\right] \tag{3}$$

where σ denotes the broadening parameter, the modified depolarization current can be written:

$$I(T) = \int_{-\infty}^{+\infty} f(E) I(T, E)\, dE \tag{4}$$

where the term $I(T,E)$ is the monoenergetic TSDC equation (see Eq. (2)).

The integral of Eq. (1) can be approximated by the following analytical expression:

$$\int_{T_0}^{T} \exp\left(-\frac{E}{kT}\right) dT = \frac{T \exp(-E/kT)(E/kT + 3.0396)}{(E/kT)^2 + 5.0364(E/kT) + 4.1916}\Bigg|_{T_0}^{T} \tag{5}$$

while the integration of Eq. (5) can be performed from 0 to $3E_0$ [16].

The picture mentioned above for the space charge polarization, is simplified. The free charge population undergoes

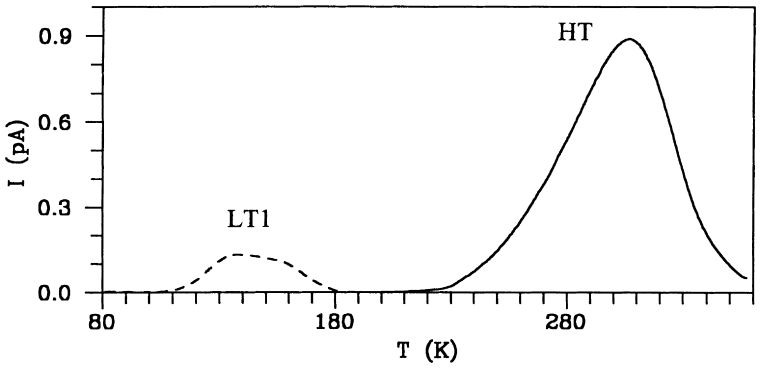

Fig. 1. Thermal depolarization spectra of polycrystalline magnesite (leukolite) by using platinum electrodes. The solid line was recorded by selecting the RT as the polarisation temperature ($T_p = 290$ K). The dashed line was recorded when $T_p = 150$ K. In both cases the external polarizing electric field intensity was $E_p = 8.33$ kV/cm and the polarization time was $t_p = 2$ min. The importance of the selection of the appropriate polarization temperature is discussed in the text.

different simultaneous processes, like the space charge limited drift, the diffusion, the neutralization to the electrodes, the creation and/or recombination of charges, etc. [18]. It is also probable that the transferring charges are trapped in internal obstacles (traps) distributed in the bulk. The space charge TSDC peaks are sensitive to the electrode material used; i.e., the blocking degree of the sample–electrode interface. The polarization state strongly depends upon the storage conditions and the electret's prehistory [15,19]. Although the competing mechanisms make impossible to construct an analytical equation for the space charge TSDC signal, rough approaches have been made and several approximate space TSDC equations have been derived [15,18,20]. The different approximations converge to the point that the initial edge of the TSDC curve coincides to that of the non-interacting rotating dipoles. Depending on the specific type of crystal, the activation energy E evaluated from space charge TSDC signals is identical to migration enthalpy h^m for the carrier diffusion, or to the migration enthalpy plus a portion of a term, which represents the association of defects [21,22].

3. Experimental details

The experiments were conducted in a cryostat, which operates from the liquid nitrogen temperature (LNT) up to 400 K. An Alcatel molecular vacuum pump maintained a vacuum better than 10^{-6} mbar. The specimens were placed between platinum electrodes. They were polarized by using a Kethley 246 DC power supply. The temperature was measured by means of a gold–chromel thermocouple and monitored by an Air-Products temperature controller. The heating rate was kept constant (around 3 K/min) during the heating stage of the TSDC run. The depolarization current was measured with a Cary 401 electrometer. A Keithley DAS 8 PGA card, which was installed into a computer, was employed to digitize the output signals from the temperature controller and the electrometer. The data were afterwards analyzed with the appropriate software we have developed.

Magnesite is the name of both single-crystal and polycrystalline $MgCO_3$ salts. The material we studied comes from the large deposits of compact polycrystalline magnesite located at the island of Euboea (Greece) [23]. The specimens were snow-like white. Because of their characteristic color, the common name for the mineral is leukolite. The typical thickness of the specimens were 1.0–1.2 mm. The analysis performed by the Institute of Geological and Mining Research (IGME, Greece) gave the following results: 47.90 wt% MgO, 2.80 wt% Si, 0.02 wt% Al, 0.13 wt% Fe, 0.41 wt% Ca, 0.02 wt% Mn, 0.02 wt% Sr, < 0.01 wt% K, 0.04 wt% Na and 0.31 wt% humidity.

4. Results and discussion

Two distinct relaxation mechanisms appear in the magnesite's thermogram (Fig. 1). The low-temperature mechanism reaches a maximum at about 140 K and is labelled LT1. The broad high-temperature band has a maximum close to room temperature (RT) and is labelled HT. The LT1 band was studied in detail in a paper published recently [4]. Therein, we proved that the LT1 mechanism is a dipolar one and is characterized by the distribution in the relaxation time. We also found that the polarization of the HT band affects the polarization state of the low temperature mechanism [4]. The same phenomenon was observed in polycrystalline dolomite ($CaMg(CO_3)_2$) [5], as well as, in some other materials [15,21]. If only the HT mechanism is unpolarized, the LT1 is recorded undisturbed. The phenomenon was interpreted in the usual manner: the total polarizing electric field intensity inside the crystal, is diminished due to the formation of the space charge. Thus, the LT1 dipoles can hardly reach a polarization state such that can actually be detected by the TSDC scheme. Even if the LT1 dipole population is

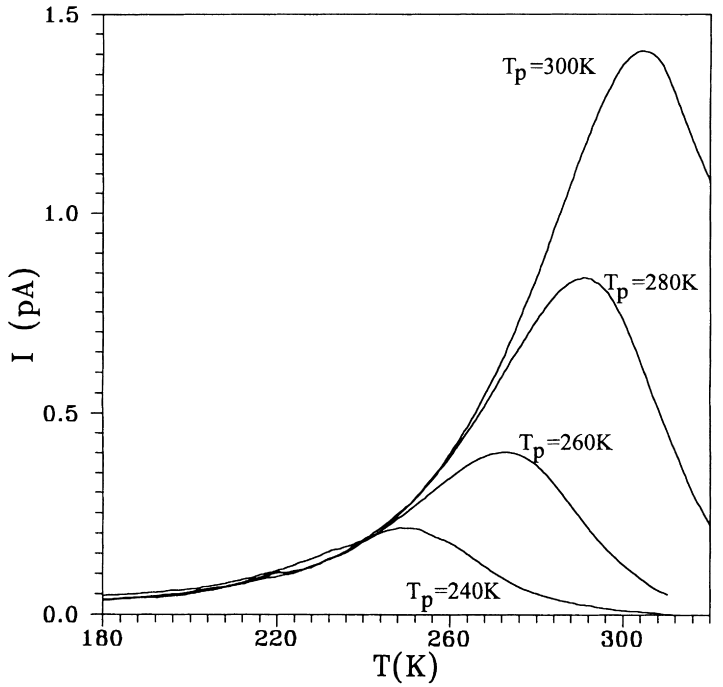

Fig. 2. Recordings of the HT band of polycrystalline magnesite, by varying the polarization temperature T_p. The polarization field intensity and the polarization time were kept constant: $E_p = 13.64$ kV/cm and $t_p = 2$ min, respectively.

polarized, their reorientation during the heating stage is affected probably by the spatial distribution of the space charge [24]. In the present paper, we focus on the study of the HT band. For extensive details and suggestions for proper dielectric characterization, see Refs. [4,5].

4.1. Dielectric characterization experiments

The TSDC thermograms, which are depicted in Fig. 2, were obtained by varying the polarization temperature T_p, while the polarization field intensity E_p and the polarization time t_p were constant ($E_p = 13.64$ kV/cm. $t_p = 2$ min). We employed platinum electrodes. On decreasing the polarization temperature, the maximum T_{max}, as well as the signal amplitude I_{max} of the HT peak, decrease gradually. The behavior may be interpreted in two different ways: (i) the HT relaxation is characterized by the distribution in the relaxation time; or (ii) the HT band is the overlap of two (or more) different peaks. The temperature T_{max} is always higher than T_p, which probably can be related to the space charge contribution.

We conducted four successive TSDC experiments, by using platinum electrodes. The polarization conditions were exactly the same; at the polarization temperature $T_p = 290$ K, we applied an electric field of intensity $E_p = 8.33$ kV/cm, for the time interval $t_p = 2$ min. The signal amplitude is gradually reduced, while the extreme variation of T_{max} is about 8 K. We also conducted five successive scans, under the same polarization conditions as those mentioned for the platinum electrodes, by employing bronze electrodes. The peak amplitude is modified, while the variation of the maximum is less than about 3 K.

In order to vary the blocking degree of the electrodes drastically, we placed a thin teflon foil between each surface of the specimen and the metal electrodes of the cryostat. This configuration is known in the literature as the MISIM (metal–insulator–sample–insulator–metal) structure [25]. The polarization conditions were the same as those mentioned above. We observe that a systematic reduction of the peak amplitude, and a slight shift to the peak maximum; i.e. less than about 3 K.

In Fig. 3, we comparatively display the thermograms recorded by using different electrode materials. We observe that the HT band exhibits moderate reproducibility. In Table 1, we depict the polarization Π_0, which was evaluated from the TSDC thermograms, reduced to the electric field intensity E_p, in relation to the electrode material. The results must be visualized critically, because the effective surface of the sample–electrode interface is different when changing the electrode material. In this sense, the results depicted in Table 1 are noticeably of the same order of magnitude. If the HT band was related to the space charge relaxation, the differences would be drastic: the use of blocking electrodes allows the rapid accumulation of free carriers and the space charge motion is embedded rapidly; hence the signal for the teflon electrodes would be much lower than that recorded

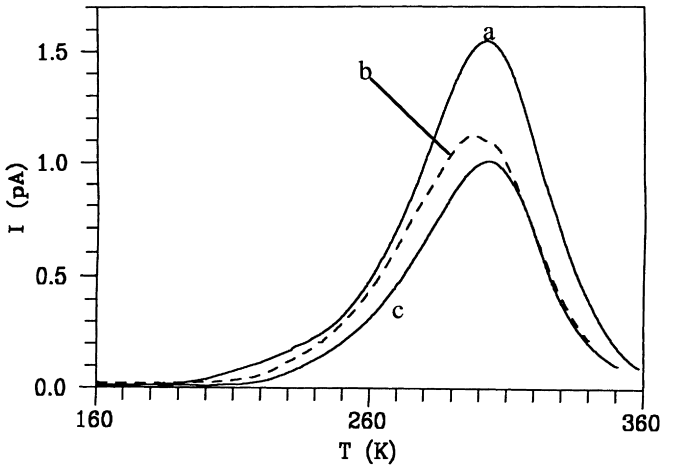

Fig. 3. Sensitivity of the HT peak on the material of the electrodes: (a) platinum, (b) teflon, (c) bronze. The polarization conditions were: T_p = 290 K, E_p = 8.33 kV/cm, t_p = 2 min. We note that the value of the external polarizing field that was applied when blocking (insulating) electrodes were employed, was carefully selected so as to achieve a field intensity in the specimen, which is practically equal to the value used when plain metal electrodes were employed.

with conductive electrodes—but this is not the case. The variations of the band's shape and the temperature where the current reaches a maximum, are slight, in comparison to the results reported for polycrystalline dolomite [8]. T_{max} does not strongly depend on the electrode nature, as it happens for a space charge dispersion. The moderate reproducibility of the HT band makes hard the attribution of the mechanism to the space charge relaxation. On the other hand, the reproducibility is much lower than we have observed for the low-temperature dipolar peaks [4–7].

For a given set of field intensity and polarization temperature, we varied the polarization time t_p. In Fig. 4, we see that the increase of the polarization time is accompanied by the augmentation of the total charge released and the shift of the maximum temperature toward higher temperatures. It seems that the saturation polarization is not achieved. As the polarization time increases, the free charges travel along longer distances. So, during the depolarization stage, the relaxation mechanism is characterized by longer relaxation times and, subsequently, the HT peak reaches its maximum at higher temperatures. However, it is risky to discuss the charge release upon the polarization time, recalling that the spatial charge population is controlled by not only the electrostatic interactions, but the charge neutralization, the diffusion, etc. The latter speculation is justified by the last thermogram presented in Fig. 4. We performed the series of experiments by starting from t_p = 2 min. After completing the set of experiments, we repeated a last experiment with t_p = 2 min again. The signal amplitude is lower than the initial one. The situation is similar to the reduction of the signal, when we perform a series of successive scans under the same polarization conditions.

We propose an explanation for the experimental results mentioned above: There are two modes for the migration of the free charge carriers: the carriers transfer along the sample toward the sample–electrode interface, or they are trapped in sites (traps) distributed into the matrix, yielding an interfacial type polarization. The carriers undergo localized transfer within the grains. Most of them are trapped at

Table 1
The polarization $\prod_0$, which was evaluated from the TSDC thermograms, reduced to the electric field intensity E_p, in function to the electrode material

Electrode material	$\frac{\Pi}{E_p}(10^{-15}\frac{C}{V\cdot mm})$
Platinum	16.33
Bronze	10.77
Teflon	9.96

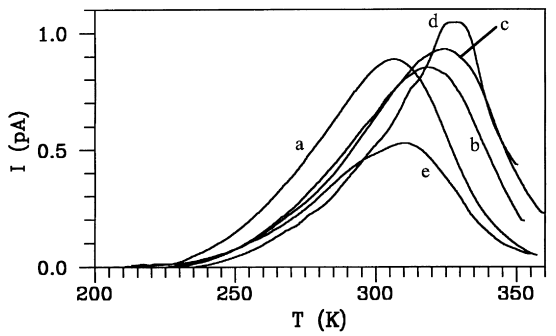

Fig. 4. Dependence of the HT band upon the polarization time interval t_p, by using platinum electrodes. The polarization conditions were: E_p = 8.33 kV/cm, T_p = 290 K and (a) t_p = 2 min, (b) t_p = 8 min, (c) t_p = 15 min, (d) t_p = 30 min, (e) t_p = 2 min (platinum electrodes).

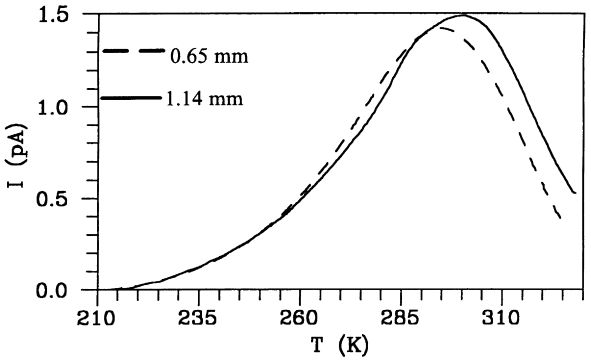

Fig. 5. Thermograms recorded by using platinum electrodes, for different values of the sample thickness. The polarization conditions were: $T_p =$ 290 K, $E_p = 26.30$ kV/cm, $t_p = 2$ min.

the grain boundaries and contribute to the interfacial polarization. The accumulation at the grain boundaries prohibits the motion of the charge population; hence a set of successive experiments lead to signals with reducing maximum (screening effect). It is probable that part of the charge population travel along distances, which are much longer than the mean grain's size. The latter are trapped at a neighboring grain boundary or they reach the sample–electrode interface. In the first case (trapping at the neighboring grain boundaries), we would observe an interfacial mechanism with longer relaxation time. This happens when the electric field is applied for long time intervals: the peak maximum shifted toward higher temperature for increasing t_p, indicating the augmentation of the relaxation time. The small portion of charges that reach the electrodes can also influence the HT band. The latter population is present as a background (i.e., multiple satellite mechanisms) to the relaxation spectrum, which compete the polarization of the HT band.

The modification of the sample's thickness provides definite information about the nature of the relaxation mechanism. We conducted a TSDC experiment on a sample of thickness 1.14 mm, under the following polarization conditions: $T_p = 290$ K, $E_p = 26.30$ kV/cm, $t_p = 2$ min. Subsequently, the sample thickness was reduced to 0.65 mm. Three days later, a TSDC run was conducted, under polarization conditions which were exactly the same as those mentioned above. In Fig. 5, the curves corresponding to the two different sample thickness values, are shown together. We note that the reduction of the sample thickness results in a slight decrease of the maximum (about 5.5 K). The signal amplitude is decreased to about 96% of the initial amplitude. The similarity between the signals corresponding to the different sample thicknesses, indicates that the HT band is related to the homogeneous polarization of the sample. The charges contributing to the HT band are immobilized at internal obstacles like the grain boundaries, and the traps (probably the grain boundaries) are spatially uniformly distributed in the matrix. At this point, it is worth noting the following: despite their potential significance in distinguishing between the homogeneous polarization and the inhomogeneous one, the experiments involving the modification of the sample thickness can hardly assist further quantitative analyses. For example, in order to ensure that the sample microstructure remains invariant, we performed the experiments by gradually reducing the thickness of the same sample. Consequently, the removal of slices during the sample thickness reduction, removes at the same time some of the space charge stored during the previous experiments.

4.2. Detection of the components of the HT peak

The selectivity is the most significant advantage of the TSDC technique; various combined polarization and depolarization modes can be conducted, in order to decompose a broad band to its constituents. The procedure is described in the literature as the thermal sampling technique [18,26,27]. In the present work, we adopt an alternative thermal sampling technique [28,29]: we chose a temperature T_{pd}, which is located within the temperature range where the TSDC peak appears. At this temperature, we polarize the sample for the time interval t_p. By keeping the temperature (T_{pd}) constant, we discharge the sample for the time interval t_d. The condition fulfilled is $t_p = t_d \equiv t_{pd}$. Immediately afterwards, the specimen is cooled to the LNT. Which is the physics hidden behind the aforementioned thermal sampling scheme? By polarizing at T_{pd}, the slow relaxation mechanisms, which activate at much higher temperatures than T_{pd}, remain practically unpolarized. The discharge at the temperature T_{pd}, results in the depolarization of the fast relaxation mechanisms, which activate at temperatures much lower than T_{pd}. Consequently, only the mechanisms activating around T_{pd} reach a detectable polarization state. In the subsequent heating stage, a band, which corresponds to the polarized mechanisms that survived the 'polarization–depolarization' procedure and represents a portion of the initial dispersion, is recorded. The thermal sampling scheme is repeated for various T_{pd} temperatures and a set of discrete responses is traced.

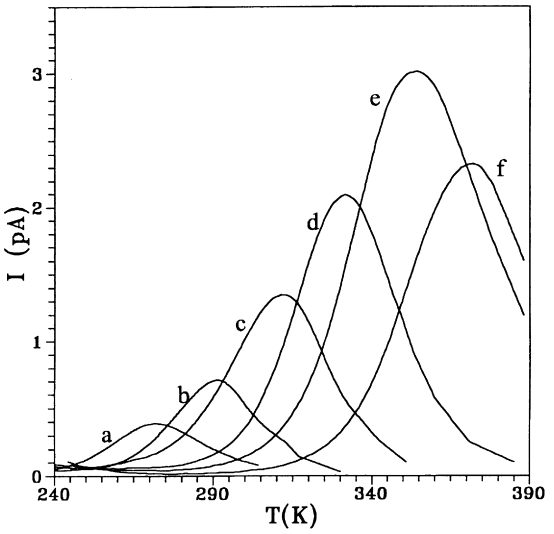

Fig. 6. Representative thermal sampling responses, so as to decompose the HT band to its components. The 'polarization–depolarization' temperatures were: (a) $T_{pd} = 250$ K, (b) $T_{pd} = 270$ K, (c) $T_{pd} = 290$ K, (d) $T_{pd} = 310$ K, (e) $T_{pd} = 330$ K, (f) $T_{pd} = 350$ K.

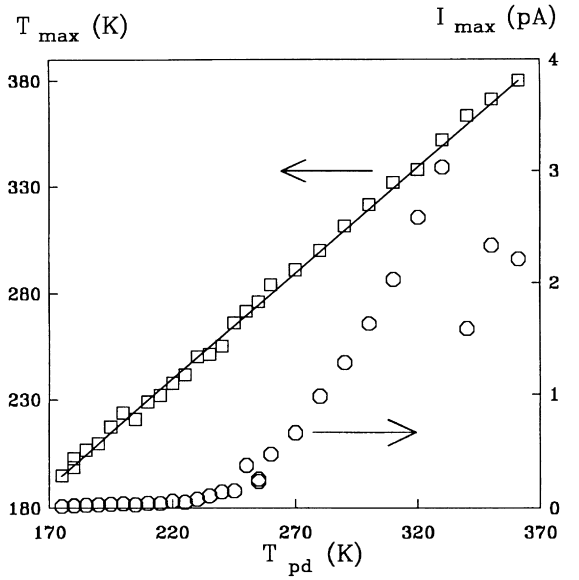

Fig. 7. Dependence of the temperature T_{max} where the thermal sampling peak reaches a maximum and its signal amplitude I_{max}, versus the 'polarization–depolarization' temperature T_{pd}.

The analysis following the thermal sampling experiments requires the construction of the $T_{max}(T_{pd})$ diagram. Provided that the TSDC peak is a single one (single relaxation time), then the maximum T_{max} of the responses would be independent of the polarization–depolarization temperature T_{pd}. If now the TSDC signal is the overlap of two single relaxation mechanisms (without distribution in their relaxation parameters), the T_{max} points would accumulate around two distinct values. The random scatter of the experimental points is typical of space charge mechanisms. The fit of a straight line with unity slope is assigned to the distribution in the relaxation time values [27,30]. The reproducibility of the thermal sampling peaks is typical of dipole contribution; on the contrary, space charge components suffer from the irreproducibility. We note that the variation of the T_{max} upon T_{pd} is, in some respects, similar to the $T_m - T_{stop}$ procedure developed for thermoluminescence analysis [31,32].

We tried 30 different T_{pd} temperatures and recorded 30 responses of the HT band. Some of the thermal sampling peaks are depicted in Fig. 6. The $T_{max}(T_{pd})$ data points lie on a straight line with slope equal to unity (Fig. 7). Consequently, the HT mechanism is characterized by the distribution in the relaxation time values. This is in accordance with the result that the maximum temperature of the HT dispersion depends on the polarization temperature T_p, when the TSDC experiments are conducted in the usual manner. We also note that the thermal sampling components reach a maximum at the temperature T_{max}, which is always higher than the 'polarization–depolarization' temperature T_{pd}. It seems quite probable that this feature is related to the space charge polarization. However, the location of any thermal sampling peak is functioned to the polarization and depolarization time intervals, as well as to the heating rate [30]. Subsequently, in our opinion, the location of the band cannot stand alone as evidence for space charge mechanisms. The thermal sampling peaks exhibit moderate reproducibility. In Fig. 7, we display additionally the peak amplitude I_{max} dependence upon T_{pd}. As T_{pd} increases, the amplitude increases gradually to a unique maximum and, at the high-temperature region, the amplitude becomes weaker. If the $I_{max}(T_{pd})$ plot exhibited two maxima, then the HT would be the overlap of two different relaxation mechanisms. The latter situation is not valid and, therefore, we conclude that the HT band is actually a unique mechanism with distribution in the relaxation parameters.

4.3. Evaluation of the relaxation parameters

The variation of the polarization temperature, when the TSDC experiments are performed in the usual experimental mode, as well as the thermal sampling technique, showed that the HT band is characterized by the distribution in the relaxation time. We performed a non-linear least-squares fit of the modified Eq. (4), whereas the distribution in the activation energy is asserted, to the experimental data. The results were visually inspected so as to verify the good match of the theoretical curve to the initial rising part of the TSDC band. In Fig. 8, a theoretical curve is depicted, together with a normalized TSDC signal. The peak was cleaned carefully from neighboring contributions, by employing the thermal sampling scheme at the polarization temperature $T_{pd} = 290$ K. The relaxation parameters of the

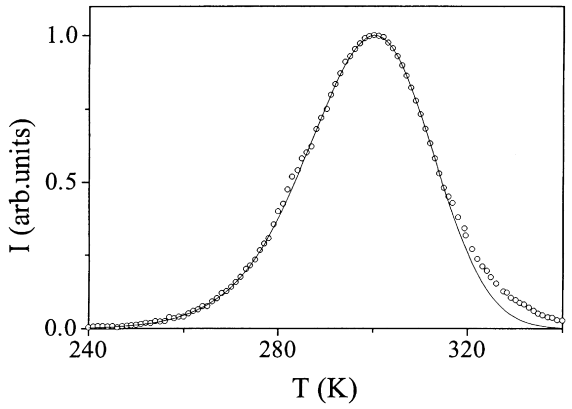

Fig. 8. Theoretical curve with Gaussian distribution in the activation energy (solid line) fitted to the experimental points (circles). The band is cleaned from neighbouring contributions by performing the thermal sampling scheme. The parameters of the theoretical curve are: $E_0 = 0.751$ eV, $\sigma = 0.020$ eV and $\tau_0 = 7.996 \times 10^{-11}$ s.

theoretical curve are: $E_0 = 0.751$ eV, $\sigma = 0.020$ eV and $\tau_0 = 7.996 \times 10^{-11}$ s.

The carriers responsible for the ionic transport are probably cation vacancies, which are the major vacancies as the result of charge compensation for the introduction of cation impurities. Aliovalent impurities with relatively small ionic radius, like K^+ or Na^+, probably contribute to the free charge diffusion within the grains of leukolite.

5. Conclusion

We studied the intense broad dispersion, which appears in the TSDC thermograms of polycrystalline magnesite at the room temperature region. The experiments indicated that the relaxation mechanism is characterized by the distribution in the relaxation time. The moderate reproducibility for a series of successive scans and the moderate dependence upon the electrode materials is probably related to an interfacial type polarization. This aspect is assisted by the similarity of the signals when the sample thickness is modified. It is probable that the moving charges are trapped at the grain boundaries. The thermal sampling scheme showed that a unique mechanism is responsible for the appearance of the broad dispersion. The relaxation parameters were evaluated by asserting that the activation energy values follow the normal distribution around a central enrage value.

References

[1] W.A. Deer, R.A. Howie, J. Zussman, An Introduction to the Rock Forming Minerals, Longman, Essex, 1966.
[2] R.J. Reeder, in: R.J. Reeder (Ed.), Crystal Chemistry of Rhombohedral Carbonates in Reviews in Mineralogy, Vol. 11, Carbonates: Mineralogy and Chemistry, Mineralogical Society of America, Washington, DC, 1983.
[3] M. Catti, A. Pavese, R. Dovesi, V.R. Saunders, Phys. Rev. B 47 (1993) 9189.
[4] A.N. Papathanassiou, J. Grammatikakis, Phys. Rev. B 56 (1997) 8590.
[5] A.N. Papathanassiou, J. Grammatikakis, Phys. Rev. B 53 (1996) 16252.
[6] N.G. Bogris, J. Grammatikakis, A.N. Papathanassiou, in: O. Kanert, J.-M. Spaeth (Eds.), Proceedings of the XII International Conference on Defects in Insulating Materials ICDIM92 (Germany, 1992), World Scientific Publishing, 1993, p. 804.
[7] A.N. Papathanassiou, J. Grammatikakis, V. Katsika, A.B. Vassilikou-Dova, Radiation Effects and Defects in Solids 134 (1995) 247.
[8] A.N. Papathanassiou, J. Grammatikakis, J. Phys. Chem. Solids 58 (1997) 1063.
[9] R. Robert, R. Barboza, G.F.L. Ferreira, M. Ferreira de Souza, Phys. Stat. Sol. (b) 59 (1973) 335.
[10] C. Bucci, R. Fieschi, Phys. Rev. Lett. 12 (1964) 16.
[11] A.N. Papathanassiou, J. Grammatikakis, Phys. Rev. B 53 (1996) 16247.
[12] A.N. Papathanassiou, Phys. Rev. B, in press.
[13] P.A. Varotsos, K.D. Alexopoulos, in: S. Amelinckx, R. Gevers, J. Nihoul (Eds.), Thermodynamics of Point Defects and Their Relation with Bulk Properties, North-Holland, Amsterdam, 1985.
[14] C. Rozluski, Acta Geophysica Polonica XLII (1995) 33.
[15] J. Vanderschueren, J. Gasiot, in: P. Braunlich (Ed.), Field Induced Thermally Stimulated Currents in Thermally Stimulated Relaxation in Solids, Springer-Verlag, Berlin, 1979.
[16] J.P. Calame, J.J. Fontanella, M.C. Wintersgill, C. Andeen, J. Appl. Phys. 58 (1985) 2811.
[17] E. Laredo, M. Puma, N. Saurez, D.R. Figueroa, Phys. Rev. B 23 (1981) 3009.
[18] J. van Turnhout, in: G.M. Sessler (Ed.), Thermally Stimulated Discharge of Polymers in Electrets, Springer-Verlag, Berlin, 1980.
[19] J. van Turnhout, in: Thermally Stimulated Discharge of Polymer Electrets, Elsevier, Amsterdam, 1975.
[20] P. Müller, Phys. Stat. Sol. (a) 23 (1974) 165.
[21] Da Yu Wang, A.S. Nowick, Phys. Stat. Sol. (a) 73 (1982) 165.
[22] I. Kunze, P. Müller, Phys. Stat. Sol. (a) 13 (1972) 197.
[23] M.H. Battey, Mineralogy for Students, Longman, London, 1981, p. 218.
[24] N. Suarez, M. Puma, E. Laredo, D. Figueroa, Cryst. Latt. Def. Amorph. Mat. 15 (1987) 283.
[25] P. Müller, Phys. Stat. Sol. (a) 67 (1981) 11.
[26] T. Nedetzka, M. Reichle, A. Mayer, H. Vogel, J. Phys. Chem. 74 (1970) 2652.
[27] M. Zielinski, Kryszewski, Journal of Electrostatics 3 (1977) 69.
[28] S. Schräder, H.-E. Carius, in: R. Gerhard-Multhaupt, W. Kunstler, L. Brehmer, R. Danz (Eds.), Berlin Proceedings of the 7th International Symposium in Electrets ISE7, 1991, p. 581.
[29] A.N. Papathanassiou, J. Grammatikakis, N. Bogris, Phys. Rev. B 48 (1993) 17715.
[30] M. Zielinski, Kryszewski, Phys. Stat. Sol. (a) 42 (1977) 305.
[31] S.W.S. McKeever, in: Thermoluminescence of Solids, Cambridge University Press, 1985, pp. 76–80.
[32] S.W.S. McKeever, Phys. Stat. Solidi (a) 62 (1980) 331.